# Complexes of Linear Carbon Clusters with Water†

**Mark Dibben, Jan Szczepanski, Christine Wehlburg, and Martin Vala***

*Department of Chemistry and The Center for Chemical Physics, University of Florida, Gainesville, Florida 32611*

*Received: October 15, 1999; In Final Form: January 21, 2000*

The complexes of linear $C_n$ ($n = 4-9$) carbon clusters with water have been formed in argon matrices and studied via FTIR spectroscopy. In most complexes, the CC stretching mode bands are shifted to the blue from the respective $C_n$ carbon cluster bands, and the OH stretching frequencies are shifted to the red. The observed shifts compare well with displacements predicted by density functional theory calculations. Isotopic $^{12}C/^{13}C$ substitution has been used to confirm the vibrational assignments of the $C_5{\cdot}H_2O$ and $C_6{\cdot}H_2O$ complexes. With higher water concentrations in the matrix, bands appear that are assigned to complexes with more than one water molecule, such as $H_2O{\cdot}C_3{\cdot}H_2O$, $C_3{\cdot}(H_2O)_2$, and $H_2O{\cdot}C_3{\cdot}(H_2O)_2$. Photolysis of the complexes leads to a number of $C_nO$ species, such as $C_5O$, $C_7O$, and $C_9O$, for which band assignments are proposed. The implications of these results for the production of molecules on grains in the interstellar medium are discussed.

## I. Introduction

Reactions of water with small carbon clusters $C_n$ ($n < 5$) in Ar matrices have been investigated previously by Ortman, Hauge, Margrave, and Kafafi.[1] These authors found that neither C ($X\ ^3P$) nor $C_2$ ($X^1\Sigma_g^+$ or $X^3\Sigma_g^-$) reacts with $H_2O$, but $C_3$ does. The $C_3{\cdot}H_2O$ complex was identified by its matrix infrared absorption at 2052 $cm^{-1}$, which was assigned to the CC stretching vibration of the complex.

Later, this assignment was confirmed by $^{13}C$-isotopic labeling.[2] In addition, photolysis of $C_3{\cdot}H_2O$ was shown to yield two intermediate photoproducts, the trans-oid and cis-oid rotomers of 3-hydroxypropadienylidene,[2] as suggested earlier by Pulay and co-workers.[3] The mechanisms of formation of the photoproducts (that is, propynal, $C_3O$, $C_2H_2$, and CO) resulting from the ultraviolet photolysis of the $C_3{\cdot}H_2O$ complex were next explained via an extensive calculation of the $C_3H_2O$ potential surface.[4]

In the present paper, we report the investigation of $C_n{\cdot}H_2O$ carbon cluster/water systems for carbon clusters up to $C_9$. For several of these complexes, weak infrared (IR) bands that are blue-shifted from the pure carbon cluster CC asymmetric stretching frequencies are observed. They are assigned to the $H_2O{\cdot}C_n{\cdot}H_2O$ species. For higher relative water concentrations (3% $H_2O$ in Ar), evidence for dimers, trimers, and higher water clusters have been observed in the OH stretching region. Density functional theory calculations of harmonic frequencies of the complexes have been performed, and they support the proposed band assignments. Finally, the production of $C_nO$ and $C_2H_2$ from the photolysis of $C_n{\cdot}H_2O$ complexes is discussed in terms of possible photochemistry in the interstellar medium.

## II. Theoretical Calculations

All calculations have been carried out using the Gaussian 94 program package.[5] Ab initio calculations were first performed using HF/6-31G(d) to calculate the probable geometries of the carbon cluster/water complexes. These initial geometries were then used as input to density functional theory (DFT) calculations using the Becke three-parameter Lee−Yang−Parr (B3LYP) functional with the 6-31G(d,p) basis set. The geometries (bond lengths and angles) were further optimized, and harmonic frequencies were calculated for $C_n{\cdot}H_2O$, $H_2O{\cdot}C_n{\cdot}H_2O$, $C_n{\cdot}(H_2O)_2$, and $H_2O{\cdot}C_n{\cdot}(H_2O)_2$ systems at the B3LYP/6-31G(d,p) level to support the proposed structures and IR band assignments.

## III. Experimental Procedures

The matrix isolation setup used in this work is similar to that described earlier in our work on the $C_3{\cdot}H_2O$ complex.[2] Briefly, pure $C_n$ carbon clusters were formed during Nd:YAG laser (532/1064 nm) ablation of pressed pellets of either $^{12}C$ or mixed powders of $^{12}C/^{13}C$. The clusters were co-deposited with Ar gas (with 1−3% $H_2O$ added) onto a CsI cryostat window (12 K). The exact concentration of $H_2O$ in the Ar matrix was unknown, principally because of the adhesion of the water molecules to the walls of the cryostat and the stainless steel transfer tubes. The mobility of $H_2O$ molecules in Ar matrices was controlled by thermal annealing of the matrix (up to 35 K), and in this manner, the concentration of $C_n{\cdot}H_2O$ complexes in the matrix was enhanced. Photodissociation of the $C_n{\cdot}H_2O$ species using a medium-pressure Hg lamp (150 W, wavelength range 250 to >900 nm, up to10 h) resulted in the appearance of new photoproducts in the matrix.

The IR absorption spectra were recorded using a Nicolet Magna 560 Fourier transform infrared spectrometer (0.25 $cm^{-1}$ resolution).

## IV. Results

Figure 1 shows the optimized geometries calculated using B3LYP/6-31G(d,p) for those carbon cluster/water complexes thought to be formed in the $C_n/Ar/H_2O$ matrices. All of the carbon clusters are very nearly linear. The water molecules are only weakly bonded to the carbon clusters, as evidenced by their long C−H bond distances. For example, in $C_3{\cdot}H_2O$, the carbon−hydrogen bond distance is 2.246 Å. As the number of

† Part of the special issue "Marilyn Jacox Festschrift".

* E-mail: mvala@chem.ufl.edu.

10.1021/jp9936906 CCC: $19.00 
Published on Web 03/09/2000

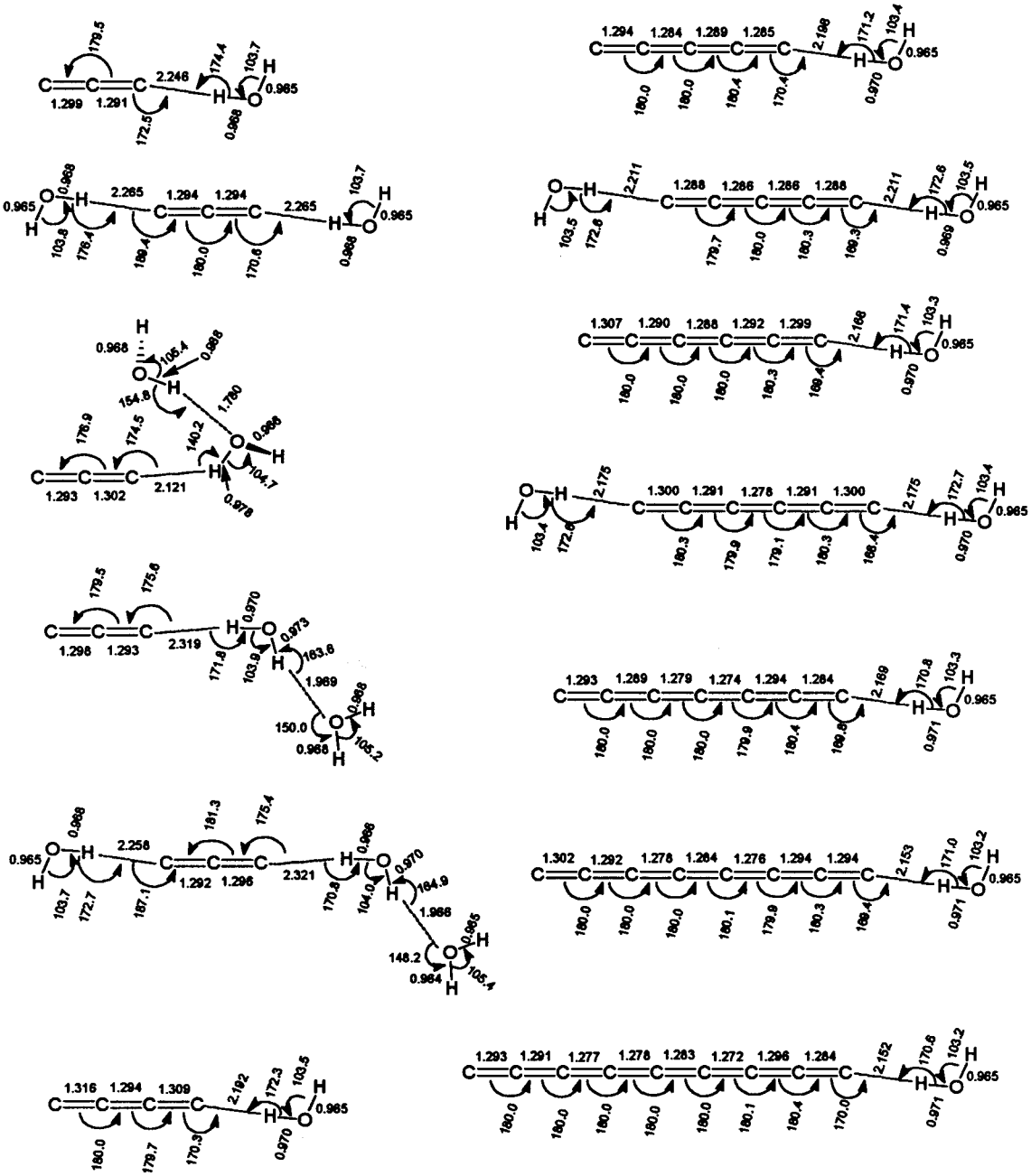

**Figure 1.** Optimized structures for the $C_n \cdot H_2O$, $H_2O \cdot C_n \cdot H_2O$, $C_n \cdot (H_2O)_2$, and $H_2O \cdot C_3 \cdot (H_2O)_2$ carbon cluster/water complexes at the B3LYP/6-31(d,p) level of theory. Bond lengths are in angstroms and angles in degrees.

carbon atoms is increased, this bond distance decreases (to 2.152 Å for $C_9 \cdot H_2O$). The weak interaction of $H_2O$ with the $C_n$ clusters is also manifested in the relatively small frequency shifts observed in the CC and OH stretching regions for the isolated vs the complexed $H_2O$ and $C_n$ molecules (see Table 1). Table 1 lists the most intense IR absorptions for the $C_n$, $C_n \cdot H_2O$, and $H_2O \cdot C_n \cdot H_2O$ ($n \leq 9$), as well as for the $C_3 \cdot (H_2O)_2$ and $H_2O \cdot C_3 \cdot (H_2O)_2$ complexes. In general, the calculated CC stretching mode intensities are higher in the $C_n \cdot H_2O$ complexes than in the corresponding pure $C_n$ clusters.

Frequency scaling factors have been used in the calculations. Only one scaling factor was used for the OH stretching and HOH bending frequencies in all of the $C_n \cdot H_2O$ and $H_2O \cdot C_n \cdot H_2O$ complexes. This factor was taken from the $C_3 \cdot H_2O$ results, for which the experimental band positions are well-known.[2] The calculated frequency of the OH asymmetric stretch was scaled to match the experimental value of 3712.7 $cm^{-1}$. Different scaling factors were used for the CC stretching vibrations in each carbon cluster and its complexes. For example, in $C_3$, $C_3 \cdot H_2O$, $H_2O \cdot C_3 \cdot H_2O$, $C_3 \cdot (H_2O)_2$, and $H_2O \cdot C_3 \cdot (H_2O)_2$, the scaling factor is from the $\nu_3$ (CC asymmetric stretching) frequency for $C_3$.

The data in the columns labeled $\Delta_{exp}$ and $\Delta_{calc}$ in Table 1 are the IR frequency differences between the carbon/water complexes and the pure carbon clusters. It is interesting to note that for $C_3 \cdot (H_2O)_2$, the calculated shift is 4.7 $cm^{-1}$ (CC asymmetric stretch), whereas for $C_3 \cdot H_2O$ and $H_2O \cdot C_3 \cdot H_2O$, it is considerably larger at 7.7 and 13.7 $cm^{-1}$, respectively.

The frequency assignments for the $C_n \cdot H_2O$ complexes are based on our observations for $C_3 \cdot H_2O$. A number of factors were considered, including the following: (1) All bands assigned to the complex grow in intensity as the $H_2O$ concentration in Ar increases. (2) During matrix annealing (to 35 K), the intensities increase for bands assigned to $C_n \cdot H_2O$, $H_2O \cdot C_n \cdot H_2O$,

**TABLE 1: Comparison of the Vibrational Frequencies for Carbon Clusters and Their Complexes with Water Observed in Ar Matrices (12 K) and Calculated at the B3LYP/6-31G(d,p) Level of Theory[m]**

| cluster | mode [j] | experimental ($cm^{-1}$) | $\Delta_{exp}$ ($cm^{-1}$) | calculated[a] ($cm^{-1}$) | $\Delta_{calc}$ ($cm^{-1}$) | cluster | mode [j] | experimental ($cm^{-1}$) | $\Delta_{exp}$ ($cm^{-1}$) | calculated[a] ($cm^{-1}$) | $\Delta_{calc}$ ($cm^{-1}$) |
|---|---|---|---|---|---|---|---|---|---|---|---|
| $C_3$ | $\nu_3$, CC asym. st. | 2039.1 | | 2039.1 [718][b] | | $H_2O{\cdot}C_5{\cdot}H_2O$ | $\nu_3^p$, CC asym. st. | 2168.4 | 4.2 | 2166.9 [2918][e] | 2.7 |
| | $\nu_1$, CC sym. st. | 1214.0 | | 1174.3 [0][b] | | | $\nu_3^p$, OH asym. st. | | | 3710.1 [284] | |
| $C_3{\cdot}H_2O$ | $\nu_3$, CC asym. st. | 2052.2 | 13.1 | 2046.8 [815][b] | 7.7 | | $\nu_1^p$, OH sym. st. | | | 3587.0 [535] | |
| | $\nu_1^p$, CC sym. st. | ~1214.5 | 0.5 | 1183.9 [2][b] | 9.6 | | $\nu_2^p$, HOH bend | | | 1601.6 [257] | |
| | $\nu_3^p$, OH asym. st. | 3712.7 | | 3712.7 [101] | | $C_6$ | $\nu_4$, CC asym. st. | 1952.5 | | 1952.5 [992][f] | |
| | $\nu_1^p$, OH sym. st. | 3598.0 | | 3595.5 [159] | | $C_6{\cdot}H_2O$ | $\nu_4^p$, CC asym. st. | 1959.2 | 6.7 | 1956.5 [1044][f] | 4.0 |
| | $\nu_2^p$, HOH bend | 1593.4 | | 1598.8 [88] | | | $\nu_5^p$, CC asym. st. | | | 1191.5 [80][f] | 8.7 |
| $H_2O{\cdot}C_3{\cdot}H_2O$ | $\nu_3^p$, CC asym. st. | 2056.2 | 17.1 | 2052.8 [926][b] | 13.7 | | $\nu_3^p$, OH asym. st. | 3703.9 | | 3704.6 [144] | |
| | $\nu_1^p$, CC sym. st. | ~1214.0[c] | 0.0 | 1193.0 [0][b] | 18.7 | | $\nu_1^p$, OH sym. st. | | | 3564.3 [354] | |
| | $\nu_3^p$, OH asym. st. | 3719.6 | | 3715.8 [219] | | | $\nu_1^p$, HOH bend | | | 1607.4 [154] | |
| | $\nu_1^p$, OH sym. st. | 3603.1 | | 3602.4 [265] | | $H_2O{\cdot}C_6{\cdot}H_2O$ | $\nu_4^p$, CC asym. st. | 1968.1 | 15.6 | 1960.1 [1059][f] | 7.6 |
| | $\nu_2^p$, HOH bend | | | 1595.0 [166] | | | $\nu_3^p$, OH asym. st. | | | 3705.9 [309] | |
| $C_3{\cdot}(H_2O)_2$[k] | $\nu_3^p$, CC asym. st. | 2051.0 | 11.9 | 2043.8 [823][b] | 4.7 | | $\nu_1^p$, OH sym. st. | | | 3568.3 [468] | |
| | $\nu_3^p$, OH asym. st. | | | 3690.1 [43] | | | $\nu_1^p$, HOH bend | | | 1603.7 [314] | |
| | $\nu_3^p$, OH asym. st. | | | 3631.9 [265] | | $C_7$ | $\nu_4$, CC asym. st. | 2128.0 | | 2128.0 [4445][g] | |
| | $\nu_1^p$, OH sym. st. | | | 3576.3 [8] | | | $\nu_5$, CC asym. st. | 1894.3 | | 1875.3 [1182][g] | |
| | $\nu_1^p$, OH sym. st. | | | 3524.4 [107] | | $C_7{\cdot}H_2O$ | $\nu_4^p$, CC asym. st. | 2127.1 | −0.9 | 2127.9 [4830][g] | −0.1 |
| | $\nu_2^p$, HOH bend | | | 1670.5 [94] | | | $\nu_5^p$, CC asym. st. | 1900.6 | 6.3 | 1883.9 [1238][g] | 8.6 |
| | $\nu_2^p$, HOH bend | | | 1617.0 [77] | | | $\nu_3^p$, OH asym. st. | 3703.9 | | 3704.4 [160] | |
| $C_3{\cdot}(H_2O)_2$[l] | $\nu_3^p$, CC asym. st. | | | 2009.7 [755][b] | | | $\nu_1^p$, OH sym. st. | | | 3564.5 [506] | |
| | $\nu_3^p$, OH asym. st. | | | 3686.2 [76] | | | $\nu_2^p$, HOH bend | | | 1609.5 [198] | |
| | $\nu_3^p$, OH asym. st. | | | 3664.3 [66] | | $C_8$ | $\nu_5$, CC asym. st. | 2071.5 | | 2071.5 [1881][h] | |
| | $\nu_1^p$, OH sym. st. | | | 3462.0 [453] | | | $\nu_6$, CC asym. st. | 1710.5 | | 1694.0 [657][h] | |
| | $\nu_1^p$, OH sym. st. | | | 3269.3 [524] | | $C_8{\cdot}H_2O$ | $\nu_5^p$, CC asym. st. | 2070.3 | −1.2 | 2072.0 [1982][h] | 0.5 |
| | $\nu_2^p$, HOH bend | | | 1602.2 [77] | | | $\nu_6^p$, CC asym. st. | 1717.0 | 6.5 | 1702.6 [641][h] | 8.6 |
| | $\nu_2^p$, HOH bend | | | 1590.5 [21] | | | $\nu_3^p$, OH asym. st. | | | 3702.5 [182] | |
| $H_2O{\cdot}C_3{\cdot}(H_2O)_2$ | $\nu_3^p$, CC asym. st. | 2053.7 | 14.6 | 2050.6 [933][b] | 11.5 | | $\nu_1^p$, OH sym. st. | | | 3553.7 [606] | |
| | $\nu_3^p$, OH asym. st. | | | 3753.7 [45] | | | $\nu_2^p$, HOH bend | | | 1610.7 [223] | |
| | $\nu_3^p$, OH asym. st. | | | 3715.7 [103] | | $C_9$ | $\nu_5$, CC asym. st. | 2078.1 | | 2075.3 [3979][i] | |
| | $\nu_3^p$, OH asym. st. | | | 3690.6 [250] | | | $\nu_6$, CC asym. st. | 1998.0 | | 1998.0 [6091][i] | |
| | $\nu_1^p$, OH sym. st. | | | 3643.1 [7] | | | $\nu_7$, CC asym. st. | 1601.0 | | 1565.5 [334][i] | |
| | $\nu_1^p$, OH sym. st. | | | 3601.7 [156] | | $C_9{\cdot}H_2O$ | $\nu_5^p$, CC asym. st. | 2081.4 | 3.3 | 2075.3 [4065][i] | 0.0 |
| | $\nu_1^p$, OH sym. st. | | | 3579.5 [141] | | | $\nu_6^p$, CC asym. st. | 2000.9 | 2.9 | 2001.1 [6708][i] | 3.1 |
| | $\nu_2^p$, HOH bend | | | 1623.3 [92] | | | $\nu_7^p$, CC asym. st. | 1607.9 | 6.9 | 1572.0 [454][i] | 6.5 |
| | $\nu_2^p$, HOH bend | | | 1597.9 [103] | | | $\nu_3^p$, OH asym. st. | | | 3702.3 [191] | |
| | $\nu_2^p$, HOH bend | | | 1570.9 [70] | | | $\nu_1^p$, OH sym. st. | | | 3553.0 [737] | |
| $C_4$ | $\nu_3$, CC asym. st. | 1543.4 | | 1543.4 [264][d] | | | $\nu_2^p$, HOH bend | | | 1613.1 [116] | |
| $C_4{\cdot}H_2O$ | $\nu_3^p$, CC asym. st. | 1550.4 | 7.0 | 1550.4 [301][d] | 7.0 | $H_2O{\cdot}C_9{\cdot}H_2O$ | $\nu_5^p$, CC asym. st. | 2088.2 | 10.1 | | |
| | $\nu_3^p$, OH asym. st. | 3706.2 | | 3707.9 [105] | | | $\nu_6^p$, CC asym. st. | 2014.2 | 16.2 | | |
| | $\nu_1^p$, OH sym. st. | | | 3576.9 [149] | | | | | | | |
| | $\nu_2^p$, HOH bend | | | 1602.4 [97] | | | | | | | |
| $C_5$ | $\nu_3$, CC asym. st. | 2164.2 | | 2164.2 [2387][e] | | | | | | | |
| | $\nu_4$, CC asym. st. | 1446.6 | | 1429.0 [112][e] | | | | | | | |
| $C_5{\cdot}H_2O$ | $\nu_3^p$, CC asym. st. | 2165.0 | 0.8 | 2165.3 [2639][e] | 1.1 | | | | | | |
| | $\nu_4^p$, CC asym. st. | 1452.9 | 6.3 | 1437.6 [111][e] | 8.6 | | | | | | |
| | $\nu_3^p$, OH asym. st. | 3706.2 | | 3708.0 [131] | | | | | | | |
| | $\nu_1^p$, OH sym. st. | | | 3580.0 [308] | | | | | | | |
| | $\nu_2^p$, HOH bend | | | 1605.2 [136] | | | | | | | |

[a] All OH stretching and HOH bending frequencies scaled by 0.9549. [b] Scaled by 0.9424. [c] Deduced from the 3262.5 $cm^{-1} = \nu_1^p + \nu_3^p$ experimental frequency (Figure 6) and the −7.7 $cm^{-1} = 2x_{13}$ anharmonicity adopted from the $C_3$ molecule, ref 7. [d] Scaled by 0.9652. [e] Scaled by 0.9510. [f] Scaled by 0.9578. [g] Scaled by 0.9414. [h] Scaled by 0.9558. [i] Scaled by 0.9362. [j] The $H_2O$ and $(H_2O)_2$ band assignments were taken from refs 21−23. [k] Planar structure (Figure 1). [l] Nonplanar structure (Figure 1). [m] Frequency shifts from the modes of pure $C_n$ carbon clusters[8−10] are given in the columns labeled Δ. Calculated intensities are given in brackets.

$C_n{\cdot}(H_2O)_2$, and $H_2O{\cdot}C_n{\cdot}(H_2O)_2$. (3) During UV photolysis, the intensities of all water and carbon cluster complex bands decrease. (4) Good agreement is found between the calculated and experimental vibrational frequencies of the $C_n{\cdot}H_2O$, $H_2O{\cdot}C_n{\cdot}H_2O$, and $C_n{\cdot}(H_2O)_2$ complexes (see Table 1). This is also true for the calculated and experimental vibrational frequencies of the $^{12}C$- and $^{13}C$-singly substituted $^{12,13}C_5{\cdot}H_2O$ and $^{12,13}C_6{\cdot}H_2O$ isotopomeric species shown in Table 2.

Many new bands are observed after photolysis (see Table 3 and Figures 2, 4, 5, 7, and 8). The photoproduct bands that increase in intensity during both annealing and photolysis (indicated by a "+" sign) have been ascribed primarily to $C_nO$ and $C_2H_2$ species.

## V. Discussion

**1. Infrared Band Assignments of Complexes.** During the past decade, intense theoretical gas-phase and matrix-phase work has established the vibrational band assignments of a number of pure carbon clusters. In the following sections, these assignments will be discussed in relation to the new positions assigned to the water complexes of these clusters. The pure carbon cluster assignments for $C_n$ ($n < 10$) are collected in an excellent review by van Orden and Saykally,[8] whereas for linear $C_{11}$ and $C_{10}/C_{12}$ clusters, the assignments are taken from new work from our lab.[9,10]

*$C_3{\cdot}(H_2O)_m$ Complexes.* The 2052.2 $cm^{-1}$ absorption band has been previously assigned to the CC asymmetric stretch vibration in the $C_3{\cdot}H_2O$ complex by Ortman et al.,[1] and this assignment was later confirmed[2] using isotopic substitution.

In Figure 2, a weak band at 2056.2 $cm^{-1}$ is observed. It is blue-shifted with respect to the $C_3{\cdot}H_2O$ band. On the basis of its calculated blue shift (see Table 1), this peak is assigned to the $H_2O{\cdot}C_3{\cdot}H_2O$ complex. The B3LYP/6-31G(d,p) frequency calculations show the dimer complex $C_3{\cdot}(H_2O)_2$ to be red-shifted compared to $C_3{\cdot}H_2O$.

**TABLE 2: Calculated [B3LYP/6-31G(d,p)] and Experimental (Ar/12 K) All-$^{12}$C-Substituted and Singly $^{13}$C-Substituted Isotopomer Frequencies for the Asymmetric $\nu_3$ and $\nu_4$ Stretching Modes of Linear $C_5$ and $C_6$ Carbon Clusters Perturbed by $H_2O$ in the $C_5{\cdot}H_2O$ and $C_6{\cdot}H_2O$ Complexes, Respectively**

| isotopomer | $\nu_{calc}$ ($cm^{-1}$) | $\nu_{exp}$ ($cm^{-1}$) | $\nu_{calc} - \nu_{exp}$ ($cm^{-1}$) |
|---|---|---|---|
| $^{12,13}C_5{\cdot}H_2O$ | | | |
| 12−12−12−12−12−1−16−1 | 2165.0[a] | 2165.0 | 0.0 |
| **13**−12−12−12−12−1−16−1 | 2162.5 | 2162.3 | 0.2 |
| 12−**13**−12−12−12−1−16−1 | 2146.5 | 2147.0 | −0.5 |
| 12−12−**13**−12−12−1−16−1 | 2131.2 | 2131.1 | 0.1 |
| 12−12−12−**13**−12−1−16−1 | 2145.8 | 2146.8 | −1.0 |
| 12−12−12−12−**13**−1−16−1 | 2162.0 | 2162.3 | −0.3 |
| 13−13−13−13−13−1−16−1 | 2080.1 | 2081.6 | −1.5 |
| **12**−13−13−13−13−1−16−1 | 2083.0 | 2084.5 | −1.5 |
| 13−**12**−13−13−13−1−16−1 | 2105.0 | 2105.6 | −0.6 |
| 13−13−**12**−13−13−1−16−1 | 2116.5 | 2118.2 | −1.7 |
| 13−13−13−**12**−13−1−16−1 | 2106.0 | 2106.0 | 0.0 |
| 13−13−13−13−**12**−1−16−1 | 2083.6 | 2084.8 | −1.2 |
| $^{12,13}C_6{\cdot}H_2O$ | | | |
| 12−12−12−12−12−12−1−16−1 | 1959.2[b] | 1959.2 | 0.0 |
| **13**−12−12−12−12−12−1−16−1 | 1955.1 | 1953.7 | 1.4 |
| 12−**13**−12−12−12−12−1−16−1 | 1935.2 | 1936.4 | −1.2 |
| 12−12−**13**−12−12−12−1−16−1 | 1950.0 | 1950.1 | −0.1 |
| 12−12−12−**13**−12−12−1−16−1 | 1949.9 | 1950.1 | −0.2 |
| 12−12−12−12−**13**−12−1−16−1 | 1932.2 | | |
| 12−12−12−12−12−**13**−1−16−1 | 1953.9 | 1953.7 | 0.2 |
| 13−13−13−13−13−13−1−16−1 | 1882.4 | 1883.8 | −1.4 |

[a] All $C_5$ complexes scaled by 0.9509. [b] All $C_6$ complexes scaled by 0.9591.

In an attempt to form $C_n$ carbon cluster/water dimer complexes, $C_n$/Ar matrixes were prepared with a high concentration of water (3% $H_2O$ added to Ar) (see Figure 3). After matrix deposition (12 K), the spectrum was similar in the CC stretch region (cf. Figure 2a), but contained stronger $C_n{\cdot}H_2O$ and $H_2O{\cdot}C_n{\cdot}H_2O$ band intensities relative to the respective $C_n$ clusters. After matrix annealing (up to 35 K), new bands associated with the $C_3$ carbon cluster band were noted at 2053.7 and 2051.0 $cm^{-1}$, blue-shifted from the $C_3$ band (see Figure 3). At a 3% water concentration, the bound OH stretch dimer band at 3573.5 $cm^{-1}$ [22] (Figure 4) increased in intensity (approximately eightfold) relative to the similar vibration in $H_2O$. At the same time, bands due to the larger water clusters grew also. These included the bands corresponding to the water trimer (3516 $cm^{-1}$), the tetramer (3374 $cm^{-1}$), the pentamer (3325 $cm^{-1}$), and possibly the hexamer (3217 $cm^{-1}$). All of these bands are broad (except that corresponding to the dimer), with shapes reminiscent of the respective water cluster bands found in jet experiments.[6]

The newly observed bands at 2053.7 and 2051.0 $cm^{-1}$ (see Figure 3) are tentatively assigned to the $C_3{\cdot}(H_2O)_2$ and $H_2O{\cdot}C_3{\cdot}(H_2O)_2$ complexes, respectively, for two reasons. First, they appear only in matrices in which the strong water dimer is also observed. Second, the positions of these bands are consistent with the calculated CC stretching frequencies of $C_3$ perturbed by $(H_2O)_2$ and by the $H_2O$ and $(H_2O)_2$ moieties. These complexes are formed mainly during annealing, probably by adding mobile $H_2O$ to the existing $C_3{\cdot}H_2O$ and $H_2O{\cdot}C_3{\cdot}H_2O$ planar systems. From the calculation for $C_3{\cdot}(H_2O)_2$, we find two possible structures on the potential surface, one planar and another nonplanar. Structural parameters for both forms are shown in Figure 1, and harmonic frequencies for the most intense bands are listed in Table 1. From inspection of Table 1 for $C_3{\cdot}(H_2O)_2$, it is seen that experimental band positions suggest a preference for the planar form over the nonplanar structure. This preference could be due to a mechanism of $C_3{\cdot}(H_2O)_2$ formation that involves the addition of $H_2O$ to the already planar $C_3{\cdot}H_2O$ system during the matrix annealing process. The $H_2O{\cdot}C_3{\cdot}(H_2O)_2$ complex is a very floppy system, and to date, only the planar structure has been found. However, the possibility of a nonplanar structure cannot be excluded.

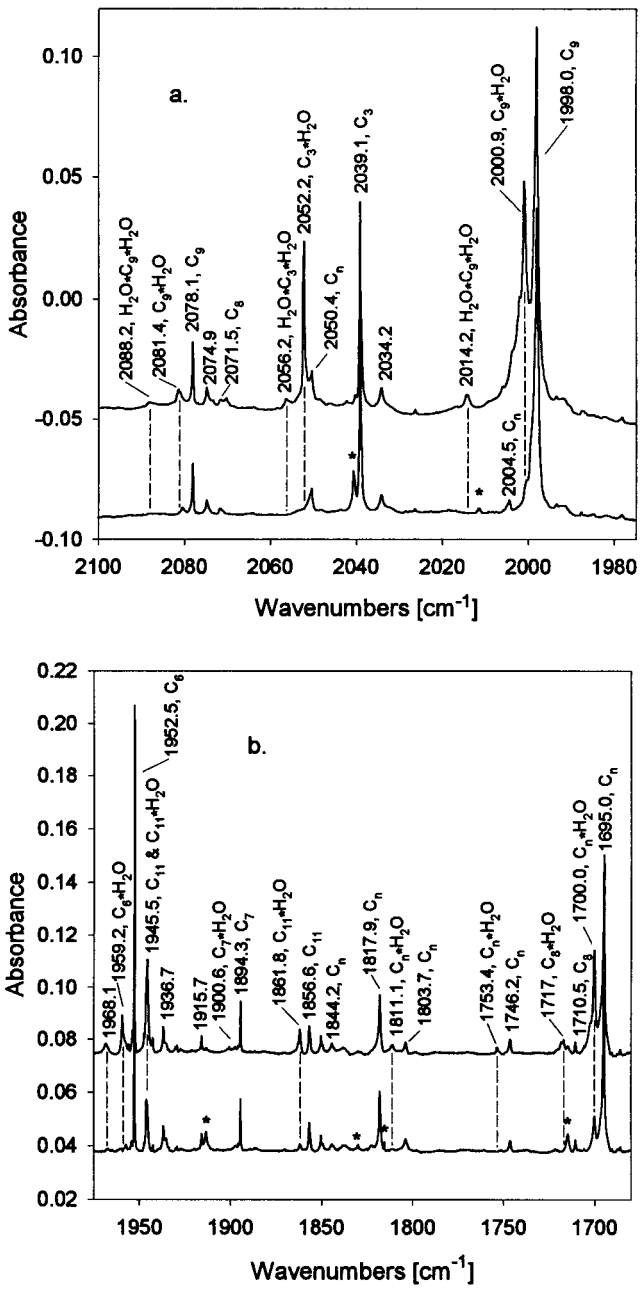


**Figure 2.** Infrared absorption spectra in the two CC stretching energy regions of $C_n$ carbon clusters and $C_n{\cdot}H_2O$ and $H_2O{\cdot}C_n{\cdot}H_2O$ carbon cluster/water complexes isolated in Ar (with 1% $H_2O$) matrices. Spectra were recorded after matrix annealing up to 35 K and cooling back to 12 K (upper spectrum) and after 10 h photolysis of the matrix using a 100-W medium-pressure Hg lamp with full spectral output (lower spectrum). The $C_n{\cdot}H_2O$ and $H_2O{\cdot}C_n{\cdot}H_2O$ complex bands are marked by dashed lines. The bands marked by stars are due to photoproducts (see text).

From laser ablation of a $^{12}C/^{13}C$ isotopic mixture followed by deposition with Ar (1% $H_2O$ added), it was possible to obtain the isotopomeric band pattern for the $\nu_1 + \nu_3$ combination band of $C_3$ perturbed by $H_2O$ (denoted as $\nu_1^p + \nu_3^p$ in Figure 6). For a $[^{12}C]/[^{13}C] = 7/1$ concentration ratio, only all-$^{12}$C-substituted and singly $^{13}$C-substituted isotopomers are expected. These are marked in Figure 6 and compared to the calculated band

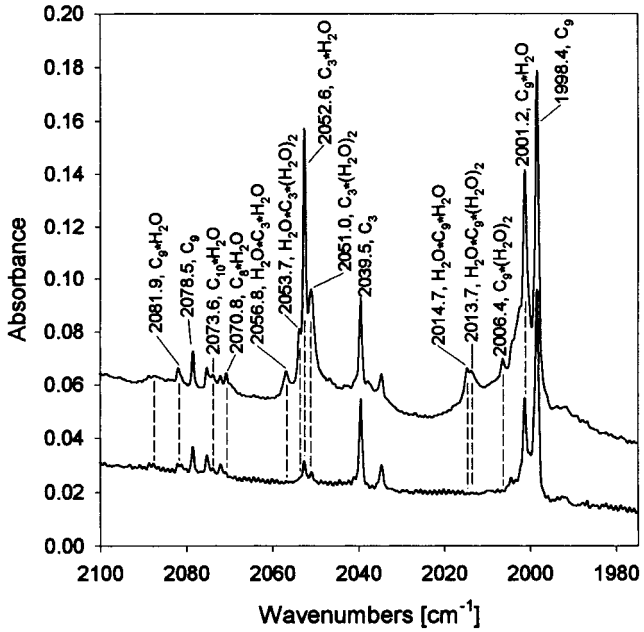


**Figure 3.** Part of the IR spectrum of carbon clusters and carbon cluster/water complexes in Ar at a high concentration of water (3% $H_2O$ added), recorded before photolysis (upper spectrum) and after 2 h of photolysis using a medium-pressure Hg lamp (lower spectrum).

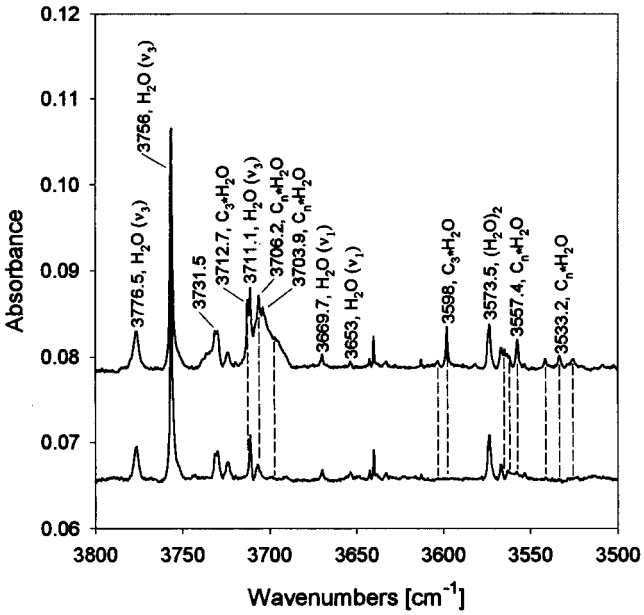


**Figure 4.** IR absorption spectrum in the O−H stretching energy region for the water/water clusters and water/carbon clusters recorded after matrix annealing (upper spectrum) and after photolysis (lower spectrum). The spectra were recorded on the same matrix as Figure 2.

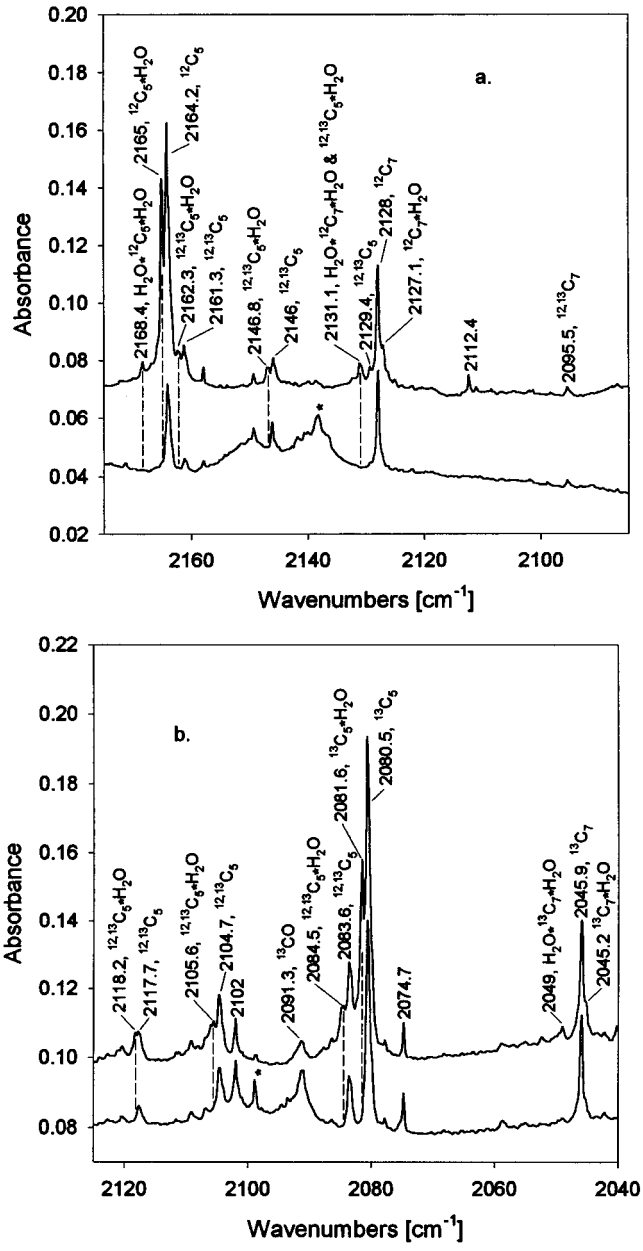


**Figure 5.** IR absorption spectra of $^{13}C$-isotopically labeled $C_5$ and $C_7$ carbon clusters and their complexes with $H_2O$, recorded for the 85% $^{12}C$ and 15% $^{13}C$ sample (spectra a) and for the 15% $^{12}C$ and 85% $^{13}C$ sample (spectra b). The upper spectra are recorded before photolysis, whereas the lower spectra were obtained after 10 h of matrix photolysis for spectra a and 6 h of matrix photolysis for spectra b with a 100-W Hg lamp. The starred band in spectra a and b is due to $^{12}CO$ and $^{13}CO$, respectively, whereas the broad band at 2149 cm$^{-1}$ is due to the $^{12}CO$•$H_2O$ complex.

positions in Table 4. The small frequency difference between the observed and calculated [B3LYP/6-31G(d,p)] isotopomeric band positions supports our assignment of the 3259.0 cm$^{-1}$ band to $C_3$•$H_2O$ with the geometry predicted by theory (Figure 1).

The assignment of the 3259.0 cm$^{-1}$ band allows $\nu_1^p$, the CC symmetrical stretching frequency in the $C_3$•$H_2O$ complex, to be deduced. The combination band in an Ar matrix is the sum of $\nu_1^p$, $\nu_3^p$, and an anharmonicity constant, $2x_{13}$. Using an anharmonicity constant of −7.7 cm$^{-1}$ (from the unperturbed $C_3$ molecule[7]) yields a $\nu_1^p$ frequency of 1214.5 cm$^{-1}$. This value is only 0.5 cm$^{-1}$ different from the experimental value of 1215.0 cm$^{-1}$ for $C_3$ in Ar.

*$C_4$•$H_2O$ Complex.* A relatively small band observed in Ar matrices at 1543.4 cm$^{-1}$ is now known to be due to the $\nu_3$ ($\sigma_u$) mode of linear $C_4$. A new band that grows in intensity with increasing water concentration is seen here at 1550.4 cm$^{-1}$. The 7 cm$^{-1}$ blue shift from the $C_4$ frequency is exactly (and probably fortuitously) just what is predicted by DFT calculations for the $\nu_3^p$ mode in the $C_4$•$H_2O$ complex (see Table 1). The 1550.4 cm$^{-1}$ band is thus assigned to the CC asymmetric stretching vibration in the $C_4$•$H_2O$ complex.

In the OH stretching region, a weak band at 3706.2 cm$^{-1}$ that is observed upon the addition of $H_2O$ to the Ar matrix gas is tentatively assigned to the $\nu_3^p$ (OH asymmetric stretching vibration) mode in the $C_4$•$H_2O$ complex. The shift from the "free" water band at 3756 cm$^{-1}$ (see Figure 4) is closely

**TABLE 3: Frequencies and Proposed Assignments for the Ar Matrix (12 K) Photosensitive Absorption Bands in the 4000−700 cm$^{-1}$ Region from $^{12}C$/Ar + $H_2O$ Experiments**

| band position ($\nu$/cm$^{-1}$) | anneal[a] | photo[a] | assignment | remarks[b] | band position ($\nu$/cm$^{-1}$) | anneal[a] | photo[a] | assignment | remarks[b] |
|---|---|---|---|---|---|---|---|---|---|
| 3712.7 | + | − | $C_3$·$H_2O$; $\nu_3^p$ (OH asym. st.) | ref 2 | 2051.0 | + | − | $C_3$·$(H_2O)_2$; $\nu_3^p$ (CC asym. st.) | T[c] |
| 3706.2 | + | − | $C_4$·$H_2O$ & $C_5$·$H_2O$; $\nu_3^p$ (OH asym. st.) | T, O[c] | 2040.7 | + | + | $C_9O$ (CC asym. st.) | P, T[c] |
| 3703.9 | + | − | $C_6$·$H_2O$ & $C_7$·$H_2O$; $\nu_3^p$ (OH asym. st.) | T, O[c] | 2014.2 | + | − | $H_2O$·$C_9$·$H_2O$; $\nu_6^p$ (CC asym. st.) | T[c] |
| 3702−3688 | + | − | $C_n$·$H_2O$ ($n > 7$); $\nu_3^p$ (OH asym. st.) | T, O[c] | 2013.7 | + | − | $H_2O$·$C_9$·$(H_2O)_2$; $\nu_5^p$ (CC asym. st.) | T[c] |
| 3603.1 | + | − | $H_2O$·$C_3$·$H_2O$; $\nu_1^p$ (OH sym. st.) | T[c] | 2011.4 | + | + | $C_nO$ (CC asym. st.) | P, T[c] |
| 3598.0 | + | − | $C_3$·$H_2O$; $\nu_1^p$ (OH sym. st.) | ref 2 | 2006.4 | + | − | $C_9$·$(H_2O)_2$; $\nu_5^p$ (CC asym. st.) | T[c] |
| 3564.9 | + | − | $C_n$·$H_2O$; $\nu_1^p$ (OH sym. st.) | T[c] | 2000.9 | + | − | $C_9$·$H_2O$; $\nu_6^p$ (CC asym. st.) | T[c] |
| 3562.0 | + | − | $C_n$·$H_2O$; $\nu_1^p$ (OH sym. st.) | T[c] | 1999.6 | − | ± | *c*-$C_3H_2O$ (CC asym. st.) | P, ref 2 |
| 3557.4 | + | − | $C_n$·$H_2O$; $\nu_1^p$ (OH sym. st.) | T[c] | 1992.5 | − | + | *t*-$C_3H_2O$ (CC asym. st.) | P, ref 2 |
| 3541.3 | + | − | $C_n$·$H_2O$; $\nu_1^p$ (OH sym. st.) | T[c] | 1969.3 | − | + | $C_2O$; (CC asym. st.) | P, ref 20 |
| 3533.2 | + | − | $C_n$·$H_2O$; $\nu_1^p$ (OH sym. st.) | T[c] | 1968.1 | + | − | $H_2O$·$C_6$·$H_2O$; $\nu_4^p$ (CC asym. st.) | T[c] |
| 3525.3 | + | − | $C_n$·$H_2O$; $\nu_1^p$ (OH sym. st.) | T[c] | 1959.2 | + | − | $C_6$·$H_2O$; $\nu_4^p$ (CC asym. st.) | T[c] |
| 3262.5 | + | − | $H_2O$·$C_3$·$H_2O$; $\nu_1^p + \nu_3^p$ (CC st.) | T[c] | 1955.7 | + | − | $C_n$·$H_2O$ (CC asym. st.) | T[c] |
| 3245.3 | + | − | $C_3$·$H_2O$; $\nu_1^p + \nu_3^p$ (CC st.) | ref 2 | 1953.7 | + | − | $C_n$·$H_2O$ (CC asym. st.) | T[c] |
| 3239.9 | + | − | $C_2H_2$·$H_2O$; (CH asym. st.) | ref 18 | 1945.6 | + | − | $C_{11}$·$H_2O$; $\nu_7^p$ (CC asym. st.) | T, O/$C_{11}$[c] |
| 2944.0 | + | − | $C_5$·$H_2O$; $\nu_2^p + \nu_3^p$ (CC st.) | ref 19 | 1913.2 | + | + | $C_nO$ (CC asym. st.) | P, T[c] |
| 2251.7 | ± | ± | $C_5O$ (CO st.) | P, T[c] | 1900.6 | + | − | $C_7$·$H_2O$; $\nu_5^p$ (CC asym. st.) | T[c] |
| 2244.2 | + | + | $C_7O$ (CO st.) | P, T[c] | 1861.8 | + | − | $C_{11}$·$H_2O$; $\nu_8^p$ (CC asym. st.) | T[c] |
| 2243.3 | ± | + | $C_3O$ (CO st.) | P, ref 12 | 1829.8 | + | + | $C_nO$ (CC asym. st.) | P, T[c] |
| 2239.5 | + | + | $C_9O$ (CO st.) | P, T[c] | 1815.3 | + | + | | P |
| 2236.9 | + | + | $C_nO$ (CO st.) | P, T[c] | 1811.1 | + | − | $C_n$·$H_2O$ (CC asym. st.) | $n > 12$, T[c] |
| 2221.6 | ± | + | $C_4O$ (CO st.) | P, ref 13 | 1753.4 | + | − | $C_n$·$H_2O$; $\nu_9^p$ (CC asym. st.) | T[c] |
| 2220.2 | + | + | $C_nO$ (CO st.) | P, T[c] | 1714.6 | + | + | $C_nO$ (CC asym. st.) | P, T[c] |
| 2214.9 | + | + | $C_nO$ (CO st.) | P, T[c] | 1700.0 | + | − | $C_n$·$H_2O$ (CC asym. st.) | T[c] |
| 2210.6 | + | + | $C_nO$ (CO st.) | P, T[c] | 1668.4 | − | + | $HC_2CHO$ | P, ref 2 |
| 2207.8 | + | + | $C_nO$ (CO st.) | P, T[c] | 1607.9 | + | − | $C_9$·$H_2O$; $\nu_7^p$ (CC asym. st.) | T, O/$H_2O$[c] |
| 2202.7 | + | + | $C_nO$ (CO st.) | P, T[c] | 1606.1 | + | − | $C_n$·$H_2O$; $\nu_2^p$ (HOH bend) | T[c] |
| 2198.3 | + | + | $C_7O$ (CC asym. st.) | P, T[c] | 1593.4 | + | − | $C_3$·$H_2O$; $\nu_2^p$ (HOH bend) | O/$H_2O$, ref 2 |
| 2168.4 | + | − | $H_2O$·$C_5$·$H_2O$; $\nu_3^p$ (CC asym. st.) | T[c] | 1589.5 | + | + | | P |
| 2165.0 | + | − | $C_5$·$H_2O$; $\nu_3^p$ (CC asym. st.) | [c] | 1588.1 | + | − | $C_n$·$H_2O$; $\nu_2^p$ (HOH bend) | T[c] |
| 2138.8 | − | + | CO | P | 1550.4 | + | − | $C_4$·$H_2O$; $\nu_3^p$ (CC asym. st.) | T[c] |
| 2131.1 | + | − | $H_2O$·$C_7$·$H_2O$; $\nu_4^p$ (CC asym. st.) | T[c] | 1477.3 | + | − | $C_n$·$H_2O$ (CC asym. st.) | $n > 12$, T[c] |
| 2127.1 | + | − | $C_7$·$H_2O$; $\nu_4^p$ (CC asym. st.) | T[c] | 1460.8 | − | ± | *t*-$C_3H_2O$ (COH bend + CH st.) | P, ref 2 |
| 2108.4 | − | + | $HC_2CHO$ (CC asym. st.) | P, ref 2 | 1452.9 | + | − | $C_5$·$H_2O$; $\nu_4^p$ (CC asym. st.) | T[c] |
| 2088.2 | + | − | $H_2O$·$C_9$·$H_2O$; $\nu_5^p$ (CC asym. st.) | T[c] | 1280.5 | − | ± | *t*-$C_3H_2O$ (COH bend + CO st.) | P, ref 2 |
| 2081.4 | + | − | $C_9$·$H_2O$; $\nu_5^p$ (CC asym. st.) | T[c] | 1254.3 | − | ± | *c*-$C_3H_2O$ (COH bend + CO st.) | P, ref 2 |
| 2080.4 | + | + | $C_nO$ (CC asym. st.) | P, T[c] | 1223.1 | − | ± | *t*-$C_3H_2O$ (HCO bend + CCH bend) | P, ref 2 |
| 2073.6 | + | − | $C_{10}$·$H_2O$; $\nu_6^p$ (CC asym. st.) | T[c] | 1016.3 | − | ± | *t*-$C_3H_2O$ (CC st. + CO st.) | P, ref 2 |
| 2070.3 | + | − | $C_8$·$H_2O$; $\nu_5^p$ (CC asym. st.) | T[c] | 940.1 | − | + | $HC_2CHO$ | P, ref 2 |
| 2056.2 | + | − | $H_2O$·$C_3$·$H_2O$; $\nu_3^p$ (CC asym. st.) | T[c] | 762.3 | − | + | | P |
| 2053.7 | + | − | $H_2O$·$C_3$·$(H_2O)_2$; $\nu_3^p$ (CC asym. st.) | T[c] | 736.5 | − | + | $C_2H_2$ (CH bend) | P |
| 2052.2 | + | − | $C_3$·$H_2O$; $\nu_3^p$ (CC asym. st.) | refs 1 and 2 | | | | | |

[a] The notation "−" or "+" indicates band intensity declines or grows during matrix annealing or during photolysis, respectively. [b] P, photolysis product band; T, tentative assignment; O, overlapped bands. [c] This work.

**TABLE 4: Calculated [B3LYP/6-31G(d,p)] and Experimental (Ar/12 K) All-$^{12}C$-Substituted and Singly $^{13}C$-Substituted Isotopomer Frequencies for $\nu_1^p+\nu_3^p$ Combination Bands of $^{12/13}C_3$ Perturbed by $H_2O$ in the $^{12/13}C_3$·$H_2O$ Complex[a]**

| isotopomer | $(\nu_1^p+\nu_3^p)_{exp}$ | $\nu_1^p{}_{calc}$ | $\nu_3^p{}_{calc}$ | $(\nu_1^p+\nu_3^p)_{calc}$ | $\Delta(\nu_1^p+\nu_3^p)_{exp-calc}$ |
|---|---|---|---|---|---|
| 12−12−12−1−16−1 | 3259.0 | 1206.8[b] | 2052.2[c] | 3259.0 | 0.0 |
| **13**−12−12−1−16−1 | 3223.8 | 1182.5 | 2040.2 | 3222.7 | 1.1 |
| 12−**13**−12−1−16−1 | 3205.2 | 1206.7 | 1999.1 | 3205.8 | −0.6 |
| 12−12−**13**−1−16−1 | 3222.9 | 1183.3 | 2038.1 | 3221.4 | 1.5 |

[a] Frequencies are in cm$^{-1}$. [b] Scaled by 0.9606. [c] Scaled by 0.9448.

predicted by the calculations (at 3707.0 cm$^{-1}$). No bands are observed that can be attributed to complexes of $C_4$ with multiple water molecules, presumably because their intensities are even smaller than the weak $C_4$ and $C_4$·$H_2O$ peaks observed in our experiments.

*$C_5$·$H_2O$ Complexes.* The $\nu_3$ and $\nu_4$ CC asymmetric stretching modes of the linear $C_5$ cluster are now known to appear at 2164.2 and 1446.6 cm$^{-1}$ (in Ar), respectively. Theory predicts the analogous modes in the $C_5$·$H_2O$ complex should fall at 2165.3 and 1437.6 cm$^{-1}$, respectively. Two water-dependent bands are observed at 2165.0 and 1452.9 cm$^{-1}$, which are assigned here to the $\nu_3^p$ and $\nu_4^p$ CC asymmetric stretching vibrations, respectively, in the $C_5$·$H_2O$ complex.

Confirmation of the assignment of the more intense 2165.0 cm$^{-1}$ band was possible using $^{12}C/^{13}C$ isotopic substitution. Laser ablation of a sample with a [$^{12}$C]/[$^{13}$C] ratio = 7/1 (and a sample with the inverse ratio) resulted in the spectra shown in Figure 5a (and 5b). For the 7/1 ratio, it is expected that only all-$^{12}C$-substituted and singly $^{13}C$-substituted isotopomers will be produced in significant concentration, whereas for the inverse 1/7 ratio, only all-$^{13}C$-substituted and singly $^{12}C$-substituted species should be observed. Comparison of the calculated positions for these isotopomers of the $C_5$·$H_2O$ complex with the observed bands (see Table 2) shows quite good agreement. The maximum discrepancy is only −1.7 cm$^{-1}$. [It should be noted that only one scaling factor (0.9509) was used for all 12 isotopomer frequencies.] This good agreement lends credence to the structure predicted from the geometry optimization for the complex, as sketched in Figure 1.

In addition, a weak band at 2168.4 cm$^{-1}$ is also observed (Figure 5a) and shows annealing and photolytic behavior that mimics other cluster/water complex bands. A band is predicted

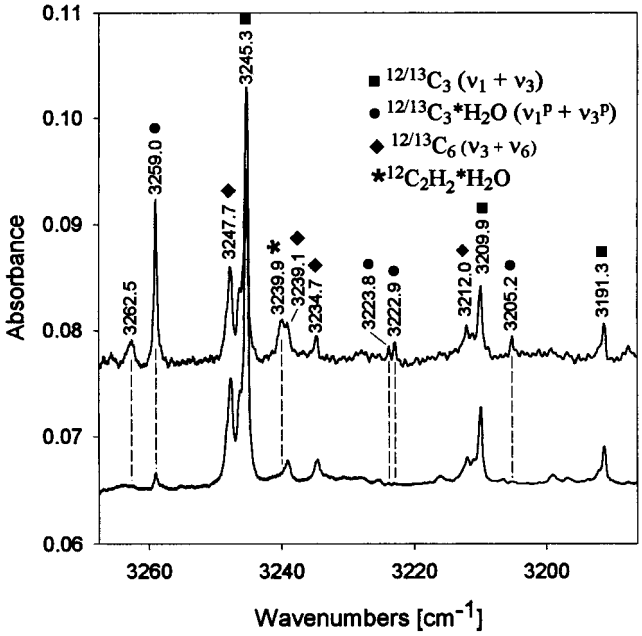


**Figure 6.** Absorption spectrum in the $\nu_1 + \nu_3$ combination band region of $^{12/13}C_3$ isotopomers (marked by filled squares). The $\nu_1^p + \nu_3^p$ combination band of $^{12/13}C_3$ modes perturbed by $H_2O$ in the $^{12/13}C_3 \cdot H_2O$ complexes are marked by filled circles. The all-$^{12}C$-substituted and singly $^{13}C$-substituted isotopomeric bands are marked. The upper spectrum was recorded before UV photolysis, whereas the lower spectrum was recorded after 2 h of photolysis using the medium-pressure Hg lamp. The 3262.5 $cm^{-1}$ band is assigned tentatively to the $\nu_1^p + \nu_3^p$ vibration in $C_3$ perturbed by water in the $H_2O \cdot C_3 \cdot H_2O$ complex.

in this region (at 2166.9 $cm^{-1}$), blue-shifted from the $C_5 \cdot H_2O$ intense band, for the double water complex $H_2O \cdot C_5 \cdot H_2O$. The 2168.4 $cm^{-1}$ band is water-concentration-dependent and is assigned to the strongest CC asymmetric stretch in this double water complex.

*$C_6 \cdot H_2O$ Complexes.* A new water-dependent band at 1959.2 $cm^{-1}$ (see Figure 2b) is assigned to the $\nu_4^p$ CC asymmetric stretching vibration in the $C_6 \cdot H_2O$ complex for the following reasons. First, for this complex, the DFT calculations predict a band at 1956.5 $cm^{-1}$, blue-shifted by 4.0 $cm^{-1}$ from the linear $C_6$ cluster peak. The observed peak is shifted slightly more (6.7 $cm^{-1}$) than predicted. Second, the comparison between calculated and experimental frequencies for the all-$^{12}C$-substituted and the singly $^{13}C$-substituted isotopomeric species (see Table 2) shows that the worst discrepancy is only 1.4 $cm^{-1}$. The small differences between observed and computed isotopomeric frequencies give good support for the band assignment of the 1959.2 $cm^{-1}$ peak to $C_6 \cdot H_2O$ and for the proposed geometry of the complex in Ar that is shown in Figure 1.

Figure 2b also shows a feature at 1968.1 $cm^{-1}$, which is assigned to the $\nu_4^p$ mode in the double water complex $H_2O \cdot C_6 \cdot H_2O$. The calculated frequency shift of this mode from the analogous mode in $C_6$ is almost twice as large as the computed shift of the same mode in $C_6 \cdot H_2O$ (that is, $\Delta_{calc} = 7.6$ vs 4.0 $cm^{-1}$). The observed frequencies show a similar, though somewhat larger, shift pattern ($\Delta\nu_{calc} = 15.6$ vs 6.7 $cm^{-1}$).

In the OH stretching region, the 3703.9 $cm^{-1}$ experimental band (Figure 4) is tentatively assigned to the $\nu_3^p$ OH asymmetric stretching vibration in $C_6 \cdot H_2O$. This compares favorably with the predicted frequency of 3704.6 $cm^{-1}$.

*$C_7 \cdot H_2O$ and $C_8 \cdot H_2O$ Complexes.* Of the complexes studied here, $C_7 \cdot H_2O$ is the smallest for which a red shift is predicted for its CC asymmetric stretching mode, compared to the analogous carbon cluster band (see Table 1). The frequency of the observed band at 2127.1 $cm^{-1}$ (Figure 5a) is in very good agreement with the predicted frequency at 2127.9 $cm^{-1}$. The other, lower-frequency CC asymmetric stretching mode ($\nu_5^p$) for this complex is found at 1900.6 $cm^{-1}$, which is reasonably close to the calculated band at 1883.9 $cm^{-1}$. A band at 3703.9 $cm^{-1}$ has been tentatively ascribed to the asymmetric OH stretch of this complex because of its proximity to the calculated band at 3704.4 $cm^{-1}$ (Table 1).

Two weak, water-dependent bands at 2070.8 and 1717.0 $cm^{-1}$ (Figures 3 and 2b), which disappear upon photolysis, are associated with the $C_8 \cdot H_2O$ complex. These peaks are assigned to the $\nu_5^p$ and $\nu_6^p$ CC asymmetric stretches, respectively. Agreement with the predicted frequency for the former mode is excellent (2072.0 $cm^{-1}$), but that for the latter mode is less satisfactory (1702.6 $cm^{-1}$).

*$C_9 \cdot H_2O$ Complexes.* The $C_9 \cdot H_2O$ complex is the largest for which calculations were performed in this work. Three asymmetric CC stretching modes are expected. Their computed frequencies lie at 2075.3 ($\nu_5^p$), 2001.1 ($\nu_6^p$), and 1572.0 $cm^{-1}$ ($\nu_7^p$), with the second band predicted to be the most intense (see Table 1). This mode is predicted to be shifted by 3.1 $cm^{-1}$ to the blue of the $C_9$ mode (at 1998.0 $cm^{-1}$). A strong band is observed in the spectrum (Figures 2a and 3) at 2000.9 $cm^{-1}$. It is photosensitive, water-dependent, and blue-shifted from the $C_9$ $\nu_6$ mode by 2.9 $cm^{-1}$. It is assigned here to the $\nu_6^p$ mode of $C_9 \cdot H_2O$. Two additional bands observed at 2081.4 and 1607.9 $cm^{-1}$ are assigned to the $\nu_5^p$ and $\nu_7^p$ modes of $C_9 \cdot H_2O$, respectively. Although their computed frequencies at 2075.3 ($\nu_5^p$) and 1572.0 $cm^{-1}$ ($\nu_p^7$) are in reasonable agreement with the observed frequencies, their shifts from the analogous $C_9$ modes are 0.0 $cm^{-1}$ (experiment found 3.3 $cm^{-1}$) and 6.5 $cm^{-1}$ (experiment found 6.9 $cm^{-1}$), respectively (see Table 1).

At 1% $H_2O$ in Ar, a complex band was observed at 2014.2 $cm^{-1}$, which grows with increasing $H_2O$ concentration and which is also photosensitive. In analogy with the $C_3/H_2O$ system of bands, this peak is tentatively ascribed to $H_2O \cdot C_9 \cdot H_2O$. To the blue of the 1998 $cm^{-1}$ ($C_9$) peak, we also expect a weak band due to the $\nu_8^p$ mode of linear $C_{12}$ perturbed by $H_2O$. In Ar matrices, the $\nu_8$ asymmetric stretching vibration mode of $C_{12}$ has an energy very close to 1998 $cm^{-1}$, and its absorption is overlapped by the strong $C_9$ band.[10] For these reasons, the experimental band assignment to the $H_2O \cdot C_9 \cdot H_2O$ cluster is tentative. At high $H_2O$ concentrations (3%), additional bands that are probably associated with $C_9$ are observed at 2006.4 and 2013.7 $cm^{-1}$. These are tentatively assigned to the $\nu_6^p$ asymmetric CC stretching modes in $C_9 \cdot (H_2O)_2$ and $H_2O \cdot C_9 \cdot (H_2O)_2$, respectively, on the basis of the expected frequency-shift trends seen in the $C_3 \cdot (H_2O)_2$ and $H_2O \cdot C_3 \cdot (H_2O)_2$ complexes.

*$C_n \cdot H_2O$ ($n > 9$) Complexes.* Table 3 lists the complex bands observed from the $C_n/H_2O/Ar$ experiments that are tentatively assigned to $C_n \cdot H_2O$ clusters with $n > 9$. These bands have been assigned using the following criteria. All are blue-shifted from the bands of their corresponding pure carbon clusters, all are $H_2O$-concentration-dependent, and all increase in intensity during annealing. Furthermore, all decrease in intensity during UV irradiation, behavior that is also exhibited by the complexes discussed above. The bands, shown in Figures 2b and 3, and their assignments are 2073.6 ($C_{10} \cdot H_2O$, $\nu_6^p$), 1945.6 ($C_{11} \cdot H_2O$, $\nu_7^p$), and 1861.8 $cm^{-1}$ ($C_{11} \cdot H_2O$, $\nu_8^p$).

**2. Photoproducts.** During UV photolysis of the carbon cluster/water complexes, new photoproduct bands increase in intensity simultaneously with a decrease in the complex band intensities (see Table 3). The $C_n$ bands do not increase in

**TABLE 5: Comparison of Calculated [BLYP/6-311G(d)] and Experimental (Ar/12 K) Vibrational Frequencies for Carbon−Oxide Clusters[a]**

| cluster | calculated[b] | experimental | remarks[c] |
|---|---|---|---|
| $C_3O$ $X^1\Sigma^+$ | 2266 [1165] | 2242.6 (1.0) | ref 12 |
| | | 2243.3 (1.0) | this work |
| $C_4O$ $X^3\Sigma^-$ | 2218 [535] | 2222 | ref 13 |
| | 1906 [317] | 1920 | ref 13 |
| $C_5O$ $X^1\Sigma^+$ | 2286 [2665] | 2251.7 (1.0) | this work, T |
| | 2150 [299] | | |
| | 1834 [348] | | |
| $C_6O$ $X^3\Sigma^-$ | 2227 [1729] | | |
| | 2073 [251] | | |
| $C_7O$ $X^1\Sigma^+$ | 2276 [2241] | 2244.2 (1.0) | this work, T |
| | 2188 [2628] | 2198.3 (0.9) | this work, T |
| | 2061 [1341] | | |
| $C_8O$ $X^3\Sigma^-$ | 2231 [3326] | | |
| | 1886 [614] | | |
| $C_9O$ $X^1\Sigma^+$ | 2273 [2170] | 2239.5 (0.3) | this work, T |
| | 2130 [7207] | 2040.7 (1.0) | this work, T |
| | 1814 [560] | | |

[a] Frequencies are in $cm^{-1}$. Integral intensities (km/mol) are given in brackets and relative intensities in parentheses. [b] Unscaled frequencies, ref 11. [c] T, tentative assignment.

intensity during irradiation, so the decline in the $C_n{\cdot}H_2O$ bands must be the result of a photorearrangment of the complex and not simply of a $C_n + H_2O$ fragmentation. From earlier studies of the $C_3{\cdot}H_2O$ complex in Ar matrixes, it was established that, during irradiation, this complex converts to 3-hydroxypropadienylidene (HP) and thence to propynal.[2] Further photoconversion of HP through several energetically favorable routes leads to the formation of $C_3O$, while photodepletion of propynal generates CO and $C_2H_2$.[4]

In the present study, the $C_n$ clusters were formed using a much higher photon flux and a more thorough annealing process, resulting in larger $C_n{\cdot}H_2O$ clusters than in the earlier $C_3{\cdot}H_2O$ study.[2] In the 2250−2190 $cm^{-1}$ (CO stretch) region (see Figures 7 and 8), many photoproduct bands appear after extensive UV photolysis (up to 10 h, medium-pressure Hg lamp, full spectral output). At the same time, a few of the photoproduct bands in the 2150−1700 $cm^{-1}$ (CC stretch) region increase in intensity as well. Their rate of growth correlates well with the band growth in the CO region. This observation indicates the photoproduction of $C_nO$ ($n > 3$) species from the $C_n{\cdot}H_2O$ complexes. Such a possibility will be discussed further below.

The harmonic vibrational frequencies for the linear $C_nO$ ($n < 10$) clusters have been calculated previously [BLYP/6-311G(d) level].[11] The most intense predicted IR $\sigma$ vibrations and their assignments are listed in Table 5. Experimental frequencies (in Ar) of 2242.6 $cm^{-1}$ for $C_3O$[12] and 2222 and 1920 $cm^{-1}$ for $C_4O$[13] were reported earlier. Tentative assignments of the photoproduct bands were made using predicted frequencies and characteristic band intensity patterns for the various modes. The experimental frequencies and their cluster assignments are 2251.7 $cm^{-1}$ for $C_5O$, 2244.2 $cm^{-1}$ (1.0) and 2198.3 $cm^{-1}$ (∼0.9) for $C_7O$, and 2239.5 $cm^{-1}$ (0.28) and 2040.7 $cm^{-1}$ (1.0) for $C_9O$. Relative band intensities are given in parentheses.

$C_5O$ has the highest calculated CO stretching frequency of all of the $C_nO$ clusters. In the spectrum (see Figures 7 and 8), the most suitable candidate for such an assignment is the 2251.7 $cm^{-1}$ band. Using a large-scale coupled-cluster calculation [CCSD(T)], Botschwina and co-workers[15] found that photodissociation of $C_5O$ into the $C_2$ ($X^1\Sigma_g^+$) and $C_3O$ ($X^1\Sigma^+$) fragments requires an energy ($D_0$) of 5.51 eV. Thus, $C_5O$ could fragment during photolysis with a Hg lamp. To test this, the matrix (containing no $C_n{\cdot}H_2O$ complexes) was photolyzed for an additional 5 h (see Figure 8). The 2251.7 $cm^{-1}$ band intensity decreased by 50%. It is now understandable why this band did not increase in intensity during 10 h of photolysis (see Figure 7). This is because there is a competition between the creation of $C_5O$ (from $C_5{\cdot}H_2O$) and the destruction of $C_5O$ by photodissociation. Interestingly, the $C_5$ bands (Figure 5a) did decrease in intensity during the long photolysis (10 h), even though the calculated CCSD(T) equilibrium dissociation energy for $C_5$ is ∼0.52 eV higher than that for $C_5O$.[15]

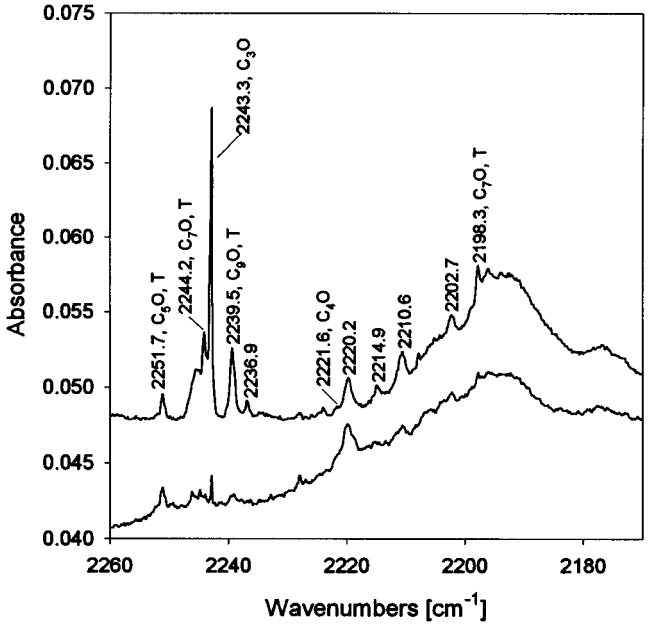


**Figure 7.** C−O stretching energy region of the spectrum presented in Figures 2 and 4. The upper spectrum is recorded after 10 h of matrix photolysis using a medium-pressure Hg lamp with full spectral output. T, tentative assignment.

More drastic photolysis effects on $C_n{\cdot}H_2O$ complexes are demonstrated in Figure 8. A relatively high yield of $C_nO$ photoproducts was observed in experiments in which the ablation laser pulse (532 nm) was set for higher power (∼40 mJ/pulse) and focused to a <1-mm-diameter spot on the graphite surface. The blue light from the Ar/$C_n$/$H_2O$ plasma region, synchronized with the molecular beam from the ablation spot, can penetrate to the matrix as well. The laser photons (single or multiple) or the plasma photons are capable of photodepleting the $C_n{\cdot}H_2O$ complexes. Figure 8 shows that all of the $C_n{\cdot}H_2O$ complex bands have disappeared and that bands that can be ascribed to various $C_nO$ species (similar in position to those in Figure 7) have been created. A band (736.5 $cm^{-1}$) due to $C_2H_2$ (acetylene) is also seen. Although it is possible under the current experimental conditions that $H_2O$ and $C_2H_2$ may photodissociate, no OH free radical band or CH stretching bands were observed (see Figures 7 and 8), except the bands due to the CH vibration in $C_2H_2$ and its complex with water. Also, no bands were observed to grow in the OH region during UV photolysis, as might be expected for simple photodecomplexation of any $C_n{\cdot}H_2O$ species. To fully understand the energetically favorable reaction routes of $C_nO$ and $C_2H_2$ photoproduction from the $C_n{\cdot}H_2O$ complexes, additional calculations will be required.

## VI. Astrophysical Implications

Many carbon-, hydrogen-, and oxygen-bearing molecules, including $C_3$, $C_5$, $H_2O$, CO, $C_2O$, $C_3O$, and $C_2H_2$, have now been identified from many different parts of interstellar space.[16] The fundamental question remains however: what is the source

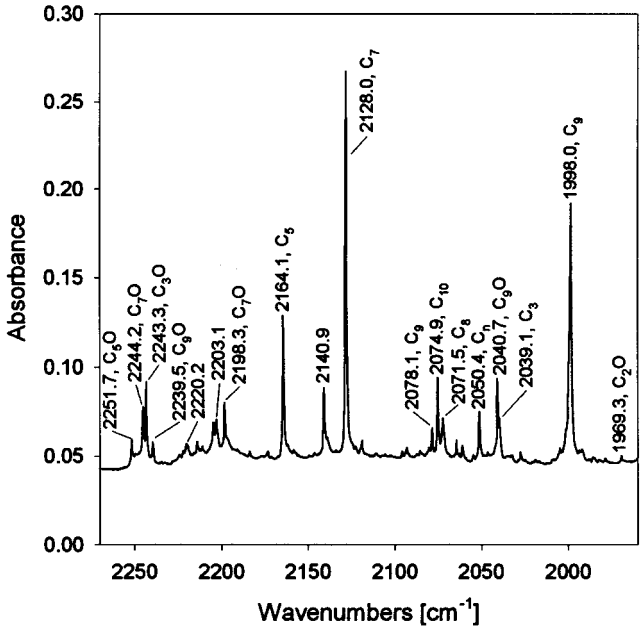


**Figure 8.** Part of the IR absorption spectrum of $^{12}C_n$ and $^{12}C_n{\cdot}H_2O$ photoproducts isolated in an Ar matrix. The matrix was prepared by laser ablation of graphite using a high flux of the 532/1064 nm photons from a Nd:YAG laser with the Ar (with 1% $H_2O$) gas excess. Radiation from the plasma region destroyed all of the $C_n{\cdot}H_2O$ complexes. Note a new group of bands in the CO stretching energy region (around 2200 cm$^{-1}$) and in the CC stretching region (below 2100 cm$^{-1}$), belonging to the $C_nO$ species.

and the mechanism of formation of these molecular species? Theoretical modeling of assumed reaction routes is not an easy task because of the existence of many variables. These include the type of reactants, the relative initial concentrations of the reactants, the reaction rate constants, and the mechanism type. The present work shows that astrophysically important species such as $C_nO$ and $C_2H_2$ can be formed from $C_n{\cdot}H_2O$ complexes exposed to UV radiation. This possibility thus extends the previously proposed model for molecule formation on the mantles of cold interstellar grains.[17] Many molecular species are expected to condense on cold grain surfaces.[18] As $H_2O$ and carbon clusters form in the envelope of carbon stars, they could be trapped on grain surfaces much as they are trapped in matrices in our experiment, thus forming $C_n{\cdot}H_2O$ complexes. After long exposures to stellar radiation, even at low photon fluxes, photorearrangement of $C_n{\cdot}H_2O$ could yield $C_nO$ and $C_2H_2$, with eventual expulsion from the grain surface into the interstellar medium.

## VII. Conclusions

Evidence is presented in this paper for the existence of complexes of linear carbon clusters, $C_n$ (with $n = 4-9$), with water. The complex band intensities are dependent on the water concentration in the matrix, as expected. CC stretching mode frequencies in most complexes are shifted to the blue, whereas the OH stretching frequencies are shifted to the red. This behavior is exactly as predicted by density functional theory calculations [B3LYP/6-31G(d,p)].

The assignments for the $C_5{\cdot}H_2O$ and $C_6{\cdot}H_2O$ complexes have been confirmed by isotopic studies using laser ablation of mixtures of $^{12}C$ and $^{13}C$. Good agreement is found between the calculated and observed isotopomeric frequencies, which in turn supports the geometries computed for the complexes. Only weak bonds appear to exist between water and the mostly linear carbon clusters. The calculated carbon−water bond distances decrease with cluster size, from 2.246 Å in $C_3{\cdot}H_2O$ to 2.152 Å in $C_9{\cdot}H_2O$.

With higher water concentrations, bands appear that are ascribed to higher multimers of water bonded to the carbon clusters. For example, in the case of $C_3$, the complexes $H_2O{\cdot}C_3{\cdot}H_2O$, $C_3{\cdot}(H_2O)_2$, and $H_2O{\cdot}C_3{\cdot}(H_2O)_2$ are tentatively assigned to specific bands.

Ultraviolet photolysis of all of the complexes leads to the formation of a number of $C_nO$ species and to a few unassigned species. Infrared band assignments are proposed for $C_5O$, $C_7O$, and $C_9O$. More extensive photolysis of the complexes results in the production of acetylene, presumably via a different photoreaction pathway.

It is suggested that the complexes of $C_n$ clusters may form with water on the mantles of small interstellar grains. Under stellar radiation, these complexes could generate the $C_nO$ species and, via a different mechanism, acetylene. Eventual expulsion from the grain and entry into the interstellar medium could follow.

**Acknowledgment.** We gratefully acknowledge the National Aeronautics and Space Administration and the Petroleum Research Foundation, administered by the American Chemical Society, for their support of this research.

## References and Notes

(1) Ortman, B. J.; Hauge, R. H.; Margrave, J. L.; Kafafi, Z. H. *J. Phys. Chem.* **1990**, *94*, 7973.
(2) Szczepanski, J.; Ekern, S.; Vala, M. *J. Phys. Chem.* **1995**, *99*, 8002.
(3) Liu, R.; Zhou, X.; Pulay, P. *J. Phys. Chem.* **1992**, *96*, 5748.
(4) Ekern, S.; Szczepanski, J.; Vala, M. *J. Phys. Chem.* **1996**, *100*, 16109.
(5) Frisch, M. J.; Trucks, G. W.; Schlegel, H. B.; Gill, P. M.; Johnson, B. G.; Robb, M. R.; Cheeseman, J. R.; Keith, T. A.; Peterson, G. A.; Montgomery, J. A.; Raghavachari, K.; Al-Laham, M. A.; Zakrzewski, V. J.; Ortiz, J. V.; Foresman, J. B.; Cioslowski, J.; Stefanov, B. B.; Nanayakkara, A.; Challacombe, M.; Peng, C. Y.; Ayala, P. Y.; Chen, W.; Wong, M. W.; Andres, J. L.; Replogle, E. S.; Gomperts, R.; Martin, R. L.; Fox, D. J.; Binkley, J. S.; Defrees, D. J.; Baker, J.; Stewart, J. P.; Head-Gordon, M.; Gonzalez, C.; Pople, J. A. *Gaussian 94*, Revision B.2; Gaussian, Inc.: Pittsburgh, PA, 1995.
(6) Paul, J. B.; Saykally, R. J. *Anal. Chem. News Features* **1997**, *69*, 287.
(7) Szczepanski, J.; Vala, M. *J. Chem. Phys.* **1993**, *99*, 7371.
(8) Van Orden, A.; Saykally, R. J. *Chem. Rev.* **1998**, *98*, 2313 and references therein.
(9) Lapinski, L.; Vala, M. *Chem. Phys. Lett.* **1999**, *300*, 195.
(10) Szczepanski, J.; Banisaukas, T. J.; Vala, M. *Chem. Phys. Lett.* In preparation.
(11) Moazzen-Ahmadi, N.; Zerbetto, F. *J. Chem. Phys.* **1995**, *103*, 6343.
(12) DeKock, R. L.; Weltner, W., Jr. *J. Am. Chem. Soc.* **1971**, *93*, 7106.
(13) Maier, G.; Reiseauer, H. P.; Schafer, U.; Balli, H. *Angew. Chem.* **1988**, *100*, 590.
(14) Reported by the Astrochemistry Working Group of Division VI (Interstellar Matter) of the International Astronomical Union. http://www.cv.nrao.edu/~awootten/allmols.html (accessed Feb 25, 2000).
(15) Botschwina, P.; Flugge, J.; Sebald, P. *J. Phys. Chem.* **1995**, *99*, 9755.
(16) Williams, D. A. *Astrophys. J.* **1968**, *151*, 935.
(17) (a) Tielens, A. G. G. M.; Hagen, W. *Astron. Astrophys.* **1982**, *114*, 245. (b) Tielens, A. G. G. M.; Allamandola, L. J. In *Interstellar Processes*; Hollenbach, D. J., Thronson, H. A., Jr., Eds.; D. Reidel: Dordrecht, The Netherlands, 1987; p 397.
(18) Farnell, L.; Radom, L. *Chem. Phys. Lett.* **1982**, *91*, 373; **1983**, *99*, 516.
(19) Fuller, J.; Szczepanski, J.; Vala, M. *Chem. Phys. Lett.* In preparation.
(20) Jacox, M. E.; Milligan, D. E.; Moll, N. G.; Thompson, W. E. *J. Chem. Phys.* **1965**, *43*, 3734.
(21) Givan, A.; Loewenschuss, A.; Nielsen, C. J. *J. Chem. Soc., Faraday Trans.* **1996**, *92*, 4927.
(22) Bentwood, R. M.; Barnes, A. J.; Orville-Thomas, W. J. *J. Mol. Spectrosc.* **1980**, *84*, 391.
(23) Person, W. B.; Del Bene, J. E.; Szajda, W.; Szczepaniak, K.; Szczesniak, M. *J. Phys. Chem.* **1991**, *95*, 2770.